Synthesis, Characterization, and Anti-Breast Cancer Properties of Cu(II) Complexes with Schiff Base and Azo Dye Ligands

Haneen Fadhil Abbas[1,2], Faris Jassim Aldoghachi[1*], Basil Abdulmahdi Saleh[1], and Yun Hin Taufiq-Yap[3,4]**

[1]*Department of Chemistry, Faculty of Science, University of Basrah, Baghdad Street, Basrah 61004, Iraq*

[2]*Department of Chemical and Petroleum Refining Engineering, College of Oil and Gas Engineering, Basra University for Oil and Gas, Altijari Street, Basrah 61001, Iraq*

[3]*Catalysis Science and Technology Research Center, Faculty of Science, University Putra Malaysia, Jl. Universiti 1, UPM Serdang, Serdang 43400, Selangor, Malaysia*

[4]*Institute of Plantation Studies, Universiti Putra Malaysia, Jl. Universiti 1, UPM Serdang, Serdang 43400, Selangor, Malaysia*

Corresponding author:

email: farisj63@gmail.com[*]; taufiq@upm.edu.my[**]

Received: January 11, 2025
Accepted: February 28, 2025

DOI: 10.22146/ijc.103683

Abstract: *This article focuses on the synthesis of three Schiff base ligands derived from 2-hydroxybenzaldehyde (B: BBr, $BOCH_3$, BNO_2) and three azo dye ligands derived from naphthol (A: ABr, $AOCH_3$, ANO_2), followed by the preparation of copper(II) complexes with these six ligands in a 1:2 (metal:ligand) ratio. The ligands and complexes were characterized by using ^{1}H-NMR, ^{13}C-NMR, FTIR, UV-vis, and ESI-MS. Thermogravimetric and differential thermal analyses of the copper complexes indicated the absence of water molecules in the crystalline coordination, demonstrating high thermal stability. The findings confirmed the formation of square-planar copper complexes. The biological activity of the complexes was evaluated on breast cancer and healthy cells using the MTT assay at different concentrations. The IC_{50} analysis showed that CuABr, CuBBr, and $CuAOCH_3$ had a significantly more substantial cytotoxic effect on cancer cells than on healthy cells. $CuBOCH_3$ and $CuBNO_2$ also exhibited notable selectivity toward cancer cells, whereas $CuANO_2$ was more toxic to normal cells. These findings highlight the potential of CuABr, CuBBr, and $CuAOCH_3$ as promising candidates for further development in targeted breast cancer therapy.*

Keywords: *metal complexes; Schiff base ligands; azo dye*

■ INTRODUCTION

Research into metal-based anticancer agents, particularly copper compounds, has gained traction following the discovery of cisplatin's effectiveness against tumors [1]. Copper compounds are appealing due to their potential as anticancer drugs with potentially fewer side effects than platinum compounds like cisplatin [2-3]. Copper ions, especially copper(I) and copper(II), possess unique redox properties that make them intriguing for cancer therapy. They can participate in redox reactions within cells, generating reactive oxygen species and inducing oxidative stress, ultimately damaging cellular components such as DNA [4]. This oxidative stress can trigger cell death pathways, making copper-based compounds promising for chemotherapy. Importantly, copper's essential role in physiological processes offers the advantage of targeting cancer cells while potentially sparing healthy cells from toxicity [5]. Nonetheless, further research is necessary to understand their mechanisms, optimize efficacy, and minimize side effects before clinical use becomes widespread.

The chemistry of Schiff base complexes, particularly those formed from aldehydes and amines, is rapidly advancing due to the diverse array of ligand structures they can form [6-7]. Schiff bases are significant due to their numerous applications in

organic synthesis and biological activity [8]. They play key roles in enzyme-catalyzed reactions like transamination, racemization, and decarboxylation. Metal complexes of Schiff bases are crucial in enzyme actions, metabolism, and transport processes [9-10]. Shi et al. [11] prepared five transition metal complexes (Cu, Ni, Co, Mn, and Fe) with Schiff base ligands derived from naphthaldehyde. They tested their anticancer activities on seven human cancer cell lines using the MTT assay. The results revealed that the copper complex exhibited the highest activity against cancer cells compared to the other prepared complexes and even surpassed cisplatin.

Azo derivatives have drawn considerable attention due to their biological activity and extensive use in medicinal chemistry. Azo dyes with a donor group positioned ortho to the azo group typically function as chelating agents. The presence of intramolecular hydrogen bonding in ortho-hydroxy naphthol azo compounds enhances their potential as chelating agents [12]. The β-naphthol azo complexes find various applications in biology, clinical practice, and analytical chemistry [13-14]. This research focuses on the synthesis of copper complexes with a square planar structure, utilizing ligands based on Schiff bases and azo dyes. It explores the spectral characteristics of both the ligands and their complexes and further examines their anticancer potential against breast cancer cell lines.

■ EXPERIMENTAL SECTION

Materials

Aniline derivatives, copper nitrate trihydrate, and toluene were purchased from Merck. The 2-naphthol and 2-hydroxy-1-naphthaldehyde were purchased from Alpha and EX-IR, respectively. Acetic acid and hydrochloric acid from BAKER. Absolute ethanol, *n*-hexane, and acetone from VWR. Human cancer cell lines were obtained from ATCC: MCF7 (HTB-22), MDA-MB-231 (HTB-26).

Instrumentation

FTIR spectra were measured using the FTIR spectrophotometer model FTIR Shimadzu, as KBr disks at room temperature and a range of 4000–400 cm^{-1}. The ^{1}H-NMR spectra of the studied compounds were scanned on a Bruker Vance 500 MHz spectrometer, whereas the ^{13}C-NMR spectra were scanned on 125 MHz. Dimethyl sulfoxide (DMSO-d_6) was used as a solvent. TGA studies were conducted using Mettler Toledo with a 10 °C/min heat rate and a range of 50–1000 °C. The electron spray ionization mass spectra (ESI-MS) of the compounds were measured by Shimadzu LC-MS 2010 A.

Procedure

Synthesis of azo dyes ligand

Azo dyes are synthesized through a diazotization-coupling reaction, which is a well-established method for forming stable azo bonds between aromatic systems. The choice of aniline derivatives in this study is based on their electronic effects, which influence the reactivity and color properties of the final azo dye. Electron-donating or withdrawing groups on the aniline ring can alter the stability of the diazonium salt, affecting yield and selectivity [15]. In a 250 mL round-bottom flask, 2 mmol of 4-bromoaniline (0.344 g), 4-methoxyaniline (0.246 g), 4-nitroaniline (0.276 g), respectively, were dissolved in 5 mL of cold water (ice bath), 2 mL of 0.03 M hydrochloric acid, and diazotized by slowly adding 0.14 g (0.2 mmol) of aqueous sodium nitrite under continuous stirring. The solution containing the diazonium salt was added dropwise to a cold solution of 0.28 g (2 mmol) of 2-naphthol in aqueous sodium hydroxide (10% w/v). The reaction mixture was stirred in an ice bath for 2–3 h, followed by TLC, separated by filtration, and washed with hot distilled water. The precipitate was recrystallized by ethanol or acetone [12,16].

Synthesis of Schiff base ligand

Schiff base ligands play a crucial role in coordination chemistry due to their ability to form stable metal complexes. The choice of 2-hydroxy-1-naphthaldehyde as a precursor is based on its ability to act as both an electron donor and a chelating agent, forming strong imine (C=N) bonds with aniline derivatives [17]. The reaction was acid-catalyzed to promote imine formation and eliminate water as a by-

product. As much as 0.344 g (1 mmol) of 2-hydroxy-1-naphthaldehyde was placed into a three-neck round flask equipped with a thermometer and condenser, stirred, and refluxed in 20 mL of absolute ethanol. Several drops of glacial acetic acid are added to the solution. After 30 min, 1 mmol of 4-bromoaniline (0.172 g), 4-methoxyaniline (0.123 g), 4-nitroaniline (0.138 g), respectively, were dissolved in 10 mL of ethanol by adding dropwise. The reaction is monitored by TLC for 2–3 h. Once completed, the resulting solution is cooled and filtered. Finally, the product is crystallized using ethanol or a mixture of acetone and water in a ratio of 9:1 [18].

Synthesis of copper(II) complex

First, 1 mmol of the ligand is placed in a three-neck round-bottom flask equipped with a thermometer, condenser, and stirrer. Depending on the ligand used, the mixture refluxed in 20 mL of absolute ethanol or acetone. During this, 10% w/v sodium hydroxide drops are added to aid the process. In the next step, 1 mmol (0.241 g) of the metal salt, dissolved in 10 mL of ethanol, is slowly added to the flask dropwise. The solution undergoes reflux for 5–6 h with TLC monitoring. Once done, the solution is cooled, and the complex is filtered, washed multiple times with ethanol or acetone, and then dried at 130 °C in an oven [19].

Cell viability assay

The 3-[4,5-dimethylthiazol-2-yl]-2,5-diphenyl tetrazolium bromide (MTT) cell viability assay was employed to assess cell growth and viability. Briefly, cells were cultured in monolayers, harvested with trypsin, and adjusted to a density of 1.4×10^4 cells per well in a 96-well plate with 200 µL of fresh medium per well. After 24 h of incubation at 37 °C with 5% CO_2, the cells were treated with varying concentrations (600–7.4 µg/mL) of the compounds for 24 h. After treatment, 200 µL of MTT solution (0.5 mg/mL in PBS or phosphate-buffered saline) was added, and the plate was incubated for 4 h at 37 °C. The supernatant was discarded, and 100 µL of DMSO was added to dissolve the formazan crystals. The plate was shaken and incubated at 37 °C until complete dissolution occurred. Cell viability was quantified by measuring the absorbance at 570 nm using a Bio Tek ELISA reader. The concentration of compounds causing 50% cell death (IC_{50}) was determined from the dose-response curves.

■ RESULTS AND DISCUSSION

Synthesis of Ligand

According to the methods used in previous studies, Schiff bases BBr, $BOCH_3$, and BNO_2, derived from 2-hydroxy-1-naphthaldehyde and substituted aniline derivatives in a 1:1 molar ratio, were synthesized in ethanol with catalytic amounts of acetic acid, as shown in Scheme 1, its physical properties are listed in Table 1. Three ligands, ABr, $AOCH_3$, and ANO_2, derived from naphthol with substituted aniline derivatives, were

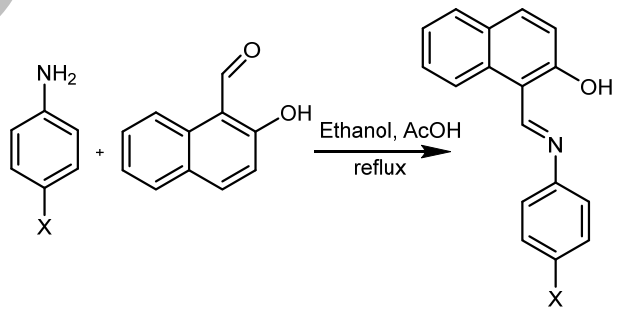

Scheme 1. Synthesis of Schiff base ligand, where X = Br, OCH_3, and NO_2

Table 1. Physical properties for the Schiff base ligand

Compounds	Name of compound	Molecular formula	Color	M.wt (g/mol)	m.p. (°C)	Yield%	R_f
BBr	(*E*)-1-(((4-bromophenyl)imino)methyl)naphthalene-2-ol	$C_{17}H_{12}BrNO$	Yellow	326.19	170	84	0.750
$BOCH_3$	(*E*)-1-(((4-methoxyphenyl)imino)methyl)naphthalene-2-ol	$C_{18}H_{15}NO_2$	Deep yellow	277.32	130	92	0.600
BNO_2	(*E*)-1-(((4-nitrophenyl)imino)methyl)naphthalene-2-ol	$C_{17}H_{12}N_2O_3$	Orange	292.29	236	86	0.512

prepared to achieve excellent yields at temperatures between 0–5 °C. The reaction involves two steps, as shown in Scheme 2. The first step involved the diazotization of aniline to form a reactive intermediate, benzene diazonium chloride while the second step involved the formation of carbanion of 2-naphthol by a nucleophilic attack initiated by the chloride ion. The nucleophilic of 2-naphthol generated then attacks the diazonium nitrogen to form the naphthol azo dye. The physical properties are listed in Table 2.

Synthesis of Copper Complexes

In this study, copper(II) complexes were prepared by reacting copper(II) nitrate hydrates with Schiff base ligands or azo dyes, synthesized in a 1:2 molar ratio (M:L) in ethanol in the presence of a basic medium of sodium hydroxide, as shown in Scheme 3. The results are summarized in Table 3.

FTIR Spectra of the Ligand and Complex

FTIR data for Schiff bases and azo dyes are presented in Table 4, while the corresponding FTIR spectra are provided in Fig. S1 and S2. The key feature of the Schiff base ligands BBr, $BOCH_3$, and BNO_2 is the appearance of a strong band corresponding to the azomethine group (C=N) in the following ranges: 1613, 1618, and 1620 cm^{-1}, respectively [20]. Meanwhile, the azo dye ligands ABr, $AOCH_3$, and ANO_2 exhibit absorption bands for the azo group (N=N) at 1485, 1451, and 1501 cm^{-1}, respectively [21]. The IR spectra of both Schiff bases and azo dyes reveal the disappearance of the phenolic hydroxyl band, which is attributed to the formation of an internal hydrogen bond between the phenolic hydrogen and the nitrogen atom of the azomethine group in Schiff bases, and the nitrogen atom of the azo group in azo dyes [22]. The aromatic (C=C) band appears in the Schiff base

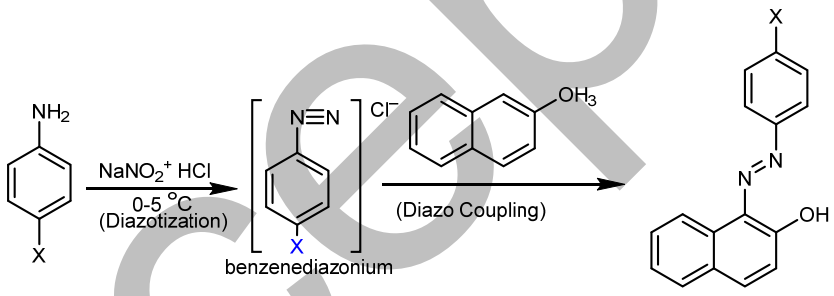

Scheme 2. Synthesis of naphthoic azo dye ligand, where X = Br, OCH_3, and NO_2

Table 2. Physical properties of the azo ligand

Compounds	Name of compound	Molecular formula	Color	M.wt (g/mol)	m.p. (°C)	Yield%	R_f
ABr	(*E*)-1-((4-bromophenyl)diazinyl)naphthalene-2-ol	$C_{16}H_{11}BrN_2O$	Red	327.16	166	96	0.675
$AOCH_3$	(*E*)-1-((4-methoxyphenyl)diazinyl)naphthalene-2-ol	$C_{17}H_{14}N_2O_2$	Dark red	278.31	130	86	0.567
ANO_2	(*E*)-1-((4-nitrophenyl)diazinyl)naphthalene-2-ol	$C_{16}H_{11}N_3O_3$	Red	293.28	250	90	0.433

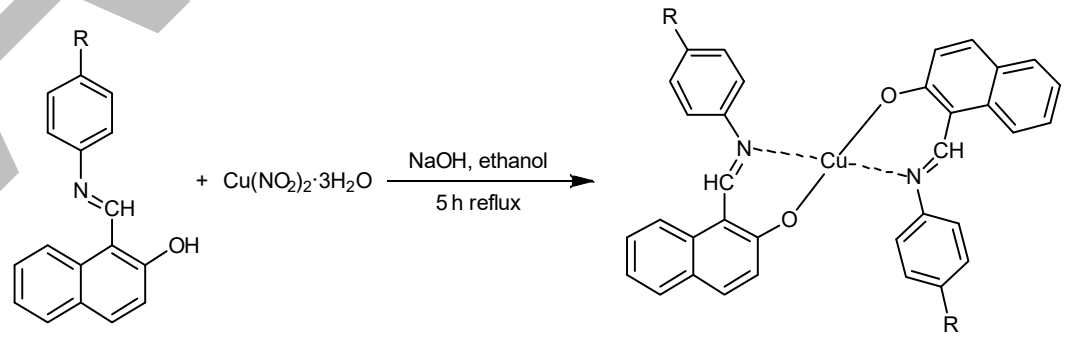

Scheme 3. Synthesis of copper complexes from Schiff base ligand

Table 3. Physical properties for the Cu-complexes

Compounds	Molecular formula	Color	Formula weight, *m/z* (found)	m.p. (°C)	Yield%
CuBBr	$[Cu(C_{17}H_{10}BrNO)_2]$	Bronze	728.95 (728.16)	320	78
$CuBOCH_3$	$[Cu(C_{18}H_{13}NO_2)_2]$	Brown	631.21 (631.21)	340	82
$CuBNO_2$	$[Cu(C_{17}H_{10}N_2O_3)_2]$	Light green	661.15 (662.85)	280	56
CuABr	$[Cu(C_{16}H_9BrN_2O)_2]$	Reddish-brown	730.93 (731.02)	350	76
$CuAOCH_3$	$[Cu(C_{17}H_{12}N_2O_2)_2]$	Reddish-brown	633.19 (633.69)	290	85
$CuANO_2$	$[Cu(C_{16}H_9N_3O_3)_2]$	Brown	663.13 (663.00)	360	60

Table 4. FTIR data for ligands

Compounds	C=N	N=N	C=C	C–H	Others
BBr	1613	-	1555	3028	600 (C–Br)
$BOCH_3$	1618	-	1572	3057	2968 (asym)–2835 (sym) of C–H in CH_3
BNO_2	1620	-	1576	3067	1502 (asym)–1332 (sym) in NO_2
ABr	-	1485	1621	3098	540 (C–Br)
$AOCH_3$	-	1501	1599	3071	2960 (asym)–2835 (sym) of C–H in CH_3
ANO_2	-	1451	1593	3067	1500.67 (asym)–1330.93 (sym) in NO_2

ligands of BBr, $BOCH_3$, and BNO_2 in the following ranges: 1555, 1572, and 1576 cm^{-1}, respectively. For the azo dye ligands ABr, $AOCH_3$, and ANO_2, the C=C aromatic band appears in the ranges of 1620 and 1599 cm^{-1}, respectively [16,23-24]. The IR spectra of the ligands $BOCH_3$ and $AOCH_3$ show symmetric and asymmetric C–H aliphatic bands due to the presence of a methoxy substituent in both ligands. Additionally, in the ligands ANO_2 and BNO_2, the spectra display bands corresponding to the NO_2 substituent, as indicated in Table 4.

Table 5 illustrates the absorption bands for the synthesized copper complexes, and the FTIR spectra are presented in Fig. S3 and S4. These spectra are characterized by a shift in the spectral range of 417–499 cm^{-1}, which is attributed to the coordination of copper with the nitrogen atom of the azomethine group in Schiff base ligands and the nitrogen atom of the azo group in azo dyes, forming a Cu–N coordination bond [25-27]. The spectra also reveal the interaction of Cu–O, where copper bonds with the oxygen atom of the phenolic group in Schiff base ligands and azo dyes, within the range of 499–586 cm^{-1}.

^{1}H- and ^{13}C-NMR Spectrum of Ligands

^{13}C-NMR spectrum of ligands

The prepared Schiff base ligands and azo dyes were characterized using ^{13}C-NMR spectroscopy. The analysis results showed several carbon atoms matching the structure of the prepared ligands. The spectra of the ligands displayed solvent for DMSO solvent exhibited a Multiple signal in the range of 39.34–40.59 ppm. The ^{13}C-NMR spectrum of the prepared Schiff bases showed a signal in the 150.09–155.79 ppm range, corresponding to the HC=N group. The spectra of the Schiff base ligands

Table 5. FTIR data for copper complexes

Compounds	C=N	N=N	C=C	C–H	M–O	M–N	Other
CuBBr	1608	-	1535	3051	499	459	584 (C–Br)
$CuBOCH_3$	1608	-	1501	3017	557	417	2949 (asym)–2835 (sym) of C–H in CH_3
$CuBNO_2$	1616	-	1533	3059	527	464	1418 (asym)–1383 (sym) in NO_2
CuABr	-	1497	1603	3051	499	453	571 (C–Br)
$CuAOCH_3$	-	1499	1601	3053	548	449	2928 (asym)–2835 (sym) of C–H in CH_3
$CuANO_2$	-	1510	1597	3065	586	455	1333 (asym)–1294 (sym) in NO_2

indicated that R substituent affects the chemical shift of the R–C_6H_4–group, as shown in Table 6, and the corresponding ^{13}C-NMR spectra are provided in Fig. S5. In the ^{13}C-NMR spectrum of the $BOCH_3$ ligand, a signal appeared at 55.65 ppm attributed to the carbon of the OCH_3 substituents. The remaining peaks in the spectrum correspond to the carbon atoms of the prepared Schiff bases.

The ^{13}C-NMR analysis results of the prepared azo dyes showed that the number of carbon atoms in the spectrum corresponds to the structure of the prepared ligands. The spectra of the ligands indicated that the effect of the R substituent on the chemical shift of the R–C_6H_4–group is evident, as shown in Table 7, and the ^{13}C-NMR spectra are provided in Fig. S6. In the ^{13}C-NMR spectrum of the $AOCH_3$ ligand, signals appeared at 55 ppm, attributed to the carbon atoms of the OCH_3 and CH_3 substituents.

^{1}H-NMR spectrum of ligand

The proton NMR spectrum of the Schiff base ligands showed a broad peak in the range of 16.01–15.24 ppm, corresponding to the hydroxyl group, and a peak in the range of 9.63–9.67 ppm attributed to HC=N group. The spectrum of the $BOCH_3$ ligand displayed a triplet at 3.79 ppm, corresponding to the OCH_3 group, as shown in Table 8. The results were consistent with those reported in previous studies [16,28-29]. The ^{1}H-NMR spectra for the ligands are provided in Fig. S7.

The NMR spectrum of the azo ligands showed a broad peak in the range of 15.69–15.05 ppm, corresponding to the hydroxyl group. The spectrum of the $BOCH_3$ ligand displayed a triplet at 3.87 ppm, corresponding to the OCH_3 group, as shown in Table 9 and the ^{1}H-NMR data of the azo dye ligands are presented in Fig. S8. The results were consistent with those reported in previous studies. The results of the FTIR, ^{1}H-NMR, and ^{13}C-NMR spectra are in good agreement with the proposed formulas

Table 6. Chemical shift (ppm) of ^{13}C-NMR Schiff base ligands

C atom	BBr	$BOCH_3$	BNO	Structure
C1	108.91	108.53	109.61	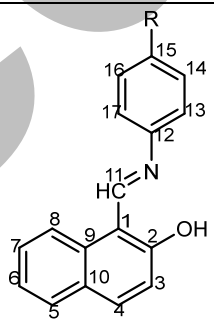
C2	168.66	169.16	172.75	
C3	118.99	121.59	121.24	
C4	129.52	133.09	133.55	
C11	155.79	153.77	150.09	
C12	133.01	136.83	156.82	
C13	123.87	121.77	124.55	
C14	132.78	115.60	125.70	
C15	121.46	158.81	145.16	
CR		55.65		

Table 7. Chemical shift (ppm) of ^{13}C-NMR azo dye ligands

C atom	ABr	$AOCH_3$	ANO	Structure
C1	128.41	128.86	128.94	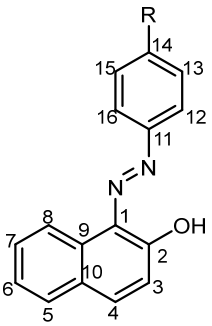
C2	169.79	157.90	179.76	
C3	120.00	121.63	126.11	
C4	140.89	142.74	144.09	
C11	144.81	136.00	148.44	
C12	121.91	123.26	117.70	
C13	133.10	115.51	122.60	
C14	121.28	161.46	144.37	
CR		56.14		

Table 8. The ^{1}H-NMR data of the Schiff base ligands

Compounds	Chemical shift (ppm)	Structure
BBr	15.55 (s, 1H) **OH**, 9.64 (s, 1H) **(CH=N)**, 7.92 (d, *J* = 9.3 Hz, 1H) **2**, 7.78 (d, *J* = 8.1 Hz, 1H) **3**, 7.58 (dd, *J* = 17.7, 9.6 Hz, 5H) **4-7-8-9-10**, 7.34 (d, *J* = 7.4 Hz, 1H) **6**, 7.02 (d, *J* = 9.0 Hz, 1H) **1**.	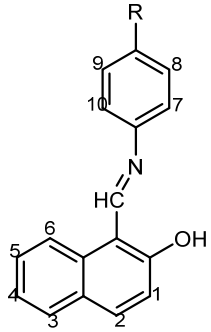
$BOCH_3$	16.01 (d, *J* = 4.4 Hz, 1H) **OH**, 9.63 (d, *J* = 4.2 Hz, 1H) **(CH=N)**, 7.89 (d, *J* = 9.2 Hz, 1H) **2**, 7.78 (d, *J* = 7.9 Hz, 1H) **3**, 7.61 (d, *J* = 8.5 Hz, 2H) **7+10**, 7.57–7.47 (m, 1H) **4**, 7.33 (t, *J* = 7.4 Hz, 1H) **5**, 7.03 (dd, *J* = 9.0, 4.2 Hz, 3H) **1+8+9**, 3.79 (s, 3H) **CH_3**.	
BNO_2	15.24 (s, 1H) **OH**, 9.67 (s, 1H) **(CH=N)**, 8.52 (d, *J* = 8.4 Hz, 1H), 8.32 (d, *J* = 8.6 Hz, 2H), 7.97 (d, *J* = 9.3 Hz, 1H) **2+4**, 7.83 (dd, *J* = 17.7, 8.3 Hz, 3H) **3+7+8**, 7.57 (t, *J* = 7.7 Hz, 1H) **5**, 7.38 (t, *J* = 7.5 Hz, 1H) **6**, 6.99 (d, *J* = 9.2 Hz, 1H) **1**.	

Table 9. The ^{1}H-NMR data of the azo dye ligands

Compounds	Chemical shift (ppm)	Structure
ABr	15.55 (s, 1H) **OH**, 8.53 (d, *J* = 8.2 Hz, 1H) **6**, 7.98 (d, *J* = 9.4 Hz, 1H) **2**, 7.88–7.81 (m, 2H) **7**-**10**, 7.79 (dd, *J* = 7.9, 1.3 Hz, 1H), 7.76–7.68 (m, 2H) **8**-**9**, 7.62 (ddd, *J* = 8.3, 7.1, 1.4 Hz, 1H) **5**, 7.47 (ddd, *J* = 8.1, 7.1, 1.2 Hz, 1H) **3**-**4**, 6.92 (d, *J* = 9.4 Hz, 1H) **1**.	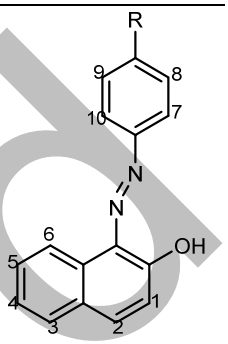
$AOCH_3$	15.05 (s, 1H) **OH**, 8.71 (d, *J* = 8.3 Hz, 1H) **6**, 7.99 (d, *J* = 9.0 Hz, 3H) **7**-**10**-**3**, 7.88 (d, *J* = 8.1 Hz, 1H) **2**, 7.67–7.60 (m, 1H) **5**, 7.50–7.43 (m, 1H) **4**, 7.14 (dd, *J* = 9.1, 2.3 Hz, 3H) **1**, 3.87 (s, 2H) **CH_3**.	
ANO_2	15.69 (s, 1H) **OH**, 8.43 (d, *J* = 7.9 Hz, 1H) **2**, 8.33 (d, *J* = 7.1 Hz, 1H) **6**, 8.03–7.90 (m, 3H) **7**-**8**-**9**-**10**, 7.73 (dd, *J* = 7.7, 1.4 Hz, 1H) **3**, 7.61 (td, *J* = 7.7, 1.4 Hz, 1H) **5**, 7.50 (td, *J* = 7.4, 1.3 Hz, 1H) **4**, 6.72 (d, *J* = 9.8 Hz, 1H) **1**.	

of the prepared ligands (Schiff bases and azo dyes) and are consistent with those reported in previous studies.

ESI-MS Spectra

The results obtained from the ESI-MS spectra of the prepared copper complexes, with molecular ion peaks for CuBBr, $CuBOCH_3$, $CuBNO_2$, CuABr, $CuAOCH_3$, and $CuNO_2$, are consistent with the proposed molecular formulas of the complexes as shown in Table 3, and the ESI-MS spectra of the complexes are provided in Fig. S9 and S10. These results confirm that the geometric structure of the synthesized copper complexes is square planar.

Thermal Analysis

Thermogravimetric analysis was conducted on copper complexes prepared using TGA and DTG techniques over a temperature range of 50 to 1000 °C, with a heating rate of 10 °C/min under an inert nitrogen atmosphere at a flow rate of 50 mL/min. Through this technique, thermal parameters such as decomposition stages, the temperature at which decomposition occurs, and the residue after decomposition were calculated.

Table 10 shows the thermal parameters derived from the thermogravimetric curves of the prepared copper complexes. The TGA dan DTG analysis of the copper complexes are shown in Fig. S11 and S12. The TGA and DTG curves for the CuBBr complex indicate that the complex decomposes in two stages. The first stage occurs in the temperature range of 60.34 to 509.95 °C, where a weight loss of 45.53% is observed, resulting from the loss of three water molecules from the crystal lattice and $C_{22}H_{18}$. The second stage occurs in the temperature range of 509.95 to 814.32 °C, with a weight loss of 24.83% due to the loss of nitrogen and bromine gases, and the remaining residue is 28.96%.

Table 10. Thermogravimetric analysis of the copper complexes

Compounds	Decom. Temp. °C			Char. contact	Mass loss (%) theoretical	Assignment
	T_i	T_{max}	T_f			
CuBBr	260.34	312.95	509.95	28.96	46.53	$3H_2O + C_{22}H_{18}$
	509.95	610.88	814.32		24.83	$Br_2 + N_2$
$CuBOCH_3$	234.42	337.92	572.57	15.33	80.90	Residue $CuCO_3$
$CuBNO_2$	211.03	285.91	572.83	21.69	75.39	Residue $CuCO_3$
CuABr	156.09	303.75	416.61	30.52	39.41	$C_{22}H_{18}$
	419.16	670.93	789.69		28.74	NO_2
$CuAOCH_3$	63.88	107.68	212.41	48.52	2.13	H_2O
	226.06	291.87	476.45		41.46	$C_{16}H_{22}$
	475.94	671.99	768.44		7.83	NO_2
$CuANO_2$	250.92	357.18	384.57	5.57	45.32	$C_{22}H_{18} + N_2$
	385.60	777.00	997.33		43.89	$NO_2 + N_2 + C_{10}H_8O$

The TGA and DTG thermogravimetric curves of the $CuBOCH_3$ complex show that it decomposes in a single stage in the temperature range of 234.42 to 572.57 °C, with a weight loss of 80.90%, and the remaining residue is 15.33%, which is CuO. The TGA and DTG curves of the $CuBNO_2$ complex indicate that it undergoes a single decomposition stage in the temperature range of 211.03 to 572.83 °C, with a weight loss of 75.39%, resulting from the decomposition of the complex, and the remaining residue is 21.69% $CuCO_3$.

The TGA and DTG curves for the CuABr complex indicate two stages of decomposition. The first stage occurs between 156.09 and 416.61 °C, with a decomposition percentage of 39.41%, caused by the loss of $C_{22}H_{18}$. The second stage takes place from 419.16 to 789.69 °C, with a 28.74% weight loss due to the release of NO_2 and Br_2. The remaining residue is 30.52%.

In contrast, the TGA curve for the $CuAOCH_3$ complex shows three decomposition stages. The first stage, from 63.86 to 212.41 °C, involves a 2.13% weight loss due to the evaporation of a water molecule from the crystal lattice. The second stage occurs between 226.06 and 467.45 °C, with a 41.46% weight loss from the loss of $C_{16}H_{22}O_2$. The third stage, from 475.94 to 768.44 °C, shows a 7.83% weight loss due to the release of NO_2. The remaining residue is 48.52%.

The TGA curve for the $CuANO_2$ complex reveals two decomposition stages. The first stage occurs between 250.92 and 384.57 °C, with a 45.32% weight loss due to the loss of $C_{22}H_{18}$ and the release of N_2 gas. The second stage, from 385.60 to 997.33 °C, shows a 43.89% weight loss due to the loss of $C_{10}H_8O$ and the release of NO_2. The remaining residue is 5.57%. The thermogravimetric analysis of the synthesized copper complexes suggests that the complexes do not contain water molecules within the coordination sphere. These findings support the proposed square planar geometry for the copper complexes.

UV-vis Spectra

In the electronic spectra of Schiff base ligands BBr, $BOCH_3$, BNO_2 and Azo dyes ligand ABr, $AOCH_3$, and ANO_2 recorded for their solutions (10^{-5} M) in ethanol or acetone, the absorption bands observed at λ_{max}, 223–335 nm were assigned to the $\pi \rightarrow \pi^*$ transitions. The bands observed in the range of λ_{max}, 340–451 nm were attributed to the $n \rightarrow \pi^*$ transitions related to HC=N and N=N groups for Schiff base [30] and azo dyes [16], respectively. Moreover, the longer wavelength band at λ_{max}, 400–481 nm was due to the characteristic intramolecular ligand-centered charge transfer (ILCT) transitions. The electronic spectra of all complexes CuBBr, $CuBOCH_3$, $CuBNO_2$, CuABr, $CuAOCH_3$, and $CuANO_2$ showed intense high energy bands at around λ_{max}, 289–340 nm and this was attributed to an intra-ligand $\pi \rightarrow \pi^*$ transitions of the coordinated ligands. The bands around λ_{max}, 440–643 nm in CuBBr, $CuBOCH_3$, and $CuANO_2$ complexes due to charge transfer from the ligand to the metal ion. In the visible domain of the absorption spectra, a band at rang λ_{max}, 519–775 nm was attributed to the d-d transitions for a Cu^{+2} complex, as it undergoes characteristic square-planar coordination [31-32]. The combined UV–vis spectra of both ligands and their copper complexes are summarized in Table 11. The UV-vis spectra of the ligands and their complexes are provided in Fig. S13 and S14.

Molar Conductivity

Table 12 shows the molar conductivity values of copper complexes, which were prepared and measured in a 10^{-3} M toluene solution at 25 °C. The results indicate that the copper complexes exhibit very low conductivity, suggesting their non-electrolytic nature, meaning that the coordination complex is non-ionic. These results support that the copper complexes prepared have a square planar geometry [32-33].

Anticancer Activity

Copper complexes have been chosen for studying their effectiveness against cancer due to their high biological activity and lower side effects compared to other complexes [34-36]. The effect of copper complexes of Schiff bases and azo compounds (CuBBr, $CuBOCH_3$, $CuBNO_2$, CuABr, $CuAOCH_3$, $CuANO_2$) was studied on human breast cancer cells (MCF-7) and normal cells (MCF10A) using the MTT assay as shown in Fig. 1 and 2.

Table 11. UV-vis spectra of the ligands and their copper complexes

Compounds	λ_{max} (nm) ligand	Transitions	λ_{max} (nm) Cu complex	Transitions
CuBBr	384	n→π*	460	d-d
	323	π→π*	440	L→Cu^{+2} (CT)
			369	n→π*
			317	π→π*
$CuBOCH_3$	392	n→π*	462	d-d
	321	π→π*	444	L→Cu^{+2} (CT)
			388	n→π*
			340	π→π*
			323	π→π*
$CuBNO_2$	400	IL (CT)	737	d-d
	340	n→π*	371	n→π*
	335	π→π*	321	π→π*
CuABr	477	n→π*	519	d-d
	305	π→π*	313	π→π*
$CuAOCH_3$	457	IL (CT)	464	d-d
	415	n→π*	417	n→π*
			289	π→π*
$CuANO_2$	481	IL (CT)	755	d-d
	223	π→π*	643	L→Cu^{+2} (CT)
			497	n→π*

Table 12. Molar conductivity of copper complexes at 10^{-3} M concentration

Complexes	Specific conductivity (10^{-6} Ω^{-1} cm^{-1})	Molar conductivity (Ω^{-1} cm^2 mol^{-1})	Type of electrolyte
CuBBr	2.40	2.40	non electrolyte
$CuBOCH_3$	1.44	1.44	non electrolyte
$CuBNO_2$	2.65	2.65	non electrolyte
CuABr	3.73	3.73	non electrolyte
$CuAOCH_3$	1.86	1.86	non electrolyte
$CuANO_2$	3.50	3.50	non electrolyte

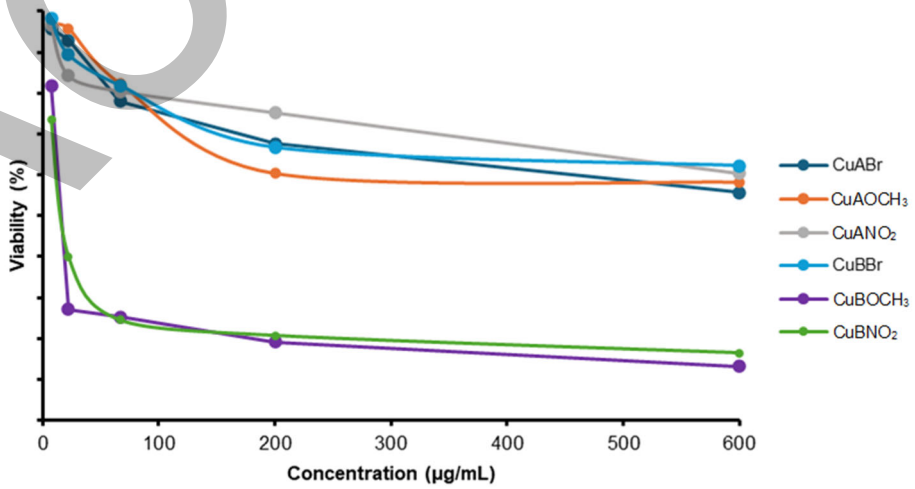

Fig 1. Effect of the concentration of copper complexes on MCF10A cell viability

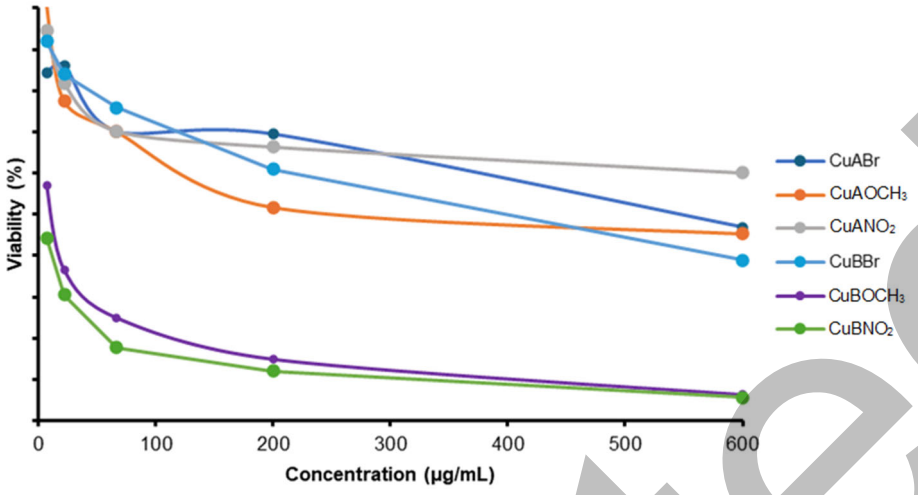

Fig 2. Effect of the concentration of copper complexes on MCF-7 cell viability

The effectiveness of copper complexes on cancerous and normal cells was evaluated after 48 h of treatment with five different concentrations (600, 200, 66.66, 22.22, and 7.4 µg/mL). Several parameters, such as viability (%), IC_{50} values, and R^2, were calculated.

The IC_{50} is a commonly used metric in pharmaceuticals and drug development to assess the effectiveness of a substance in inhibiting a biological or biochemical process [37-38]. It refers to the lowest concentration of a substance required to inhibit or kill 50% of the target cells. A lower IC_{50} value indicates a stronger inhibitory effect, while a higher IC_{50} value suggests weaker effectiveness [39-40]. In this study, the IC_{50} values for the selected copper complexes were calculated using GraphPad Prism software. The data presented in (Table 13) highlight the inhibitory effects of the copper complexes on MCF-7 cancer cells and MCF10A normal cells, along with the corresponding correlation coefficient.

The results above show that the copper complexes used clearly affect cancer cells, with their ability to inhibit cancer cell growth varying in effectiveness. Statistical analysis of the IC_{50} results indicates that the copper complexes CuABr, CuBBr, and $CuAOCH_3$ have a significantly higher effect on cancer cells compared to normal cells. On the other hand, the complexes $CuBOCH_3$ and $CuBNO_2$ exhibited a greater effect on cancer cells than on normal cells, with statistically significant differences. However, the $CuANO_2$ complex had a stronger effect on normal cells than on cancer cells. As seen from the p-value in Table 13, there are statistically significant and highly significant differences between the effects of the complexes on cancer cells versus normal cells, with very low error margins. The results shown in Table 14 indicate that the R^2 regression value demonstrates a strong relationship between the effectiveness of the complexes in killing cancer cells and

Table 13. The calculated IC_{50} of copper complexes against human breast cancer cells and normal cells

Complexes	IC_{50} (µM)		Adjusted p-value
	MDA-MB-231	MCF10A	
CuABr	196.80	57.99	0.0003
$CuAOCH_3$	106.00	41.65	0.0015
$CuANO_2$	29.89	76.74	0.0008
CuBBr	370.60	91.45	0.0017
$CuBOCH_3$	27.60	17.40	0.0174
$CuBNO_2$	17.76	1.81	0.0221

Table 14. R^2 of copper complexes against human breast cancer cells and normal cells

Complexes	R^2	
	MDA-MB-231	MCF10A
CuABr	0.9597	0.9742
$CuAOCH_3$	0.9892	0.9393
$CuANO_2$	0.9518	0.9748
CuBBr	0.9566	0.9487
$CuBOCH_3$	0.977	0.6856
$CuBNO_2$	0.9453	0.8041

Table 15. Comparison of IC_{50} values for synthesized and previously reported Cu(II) complexes in various cytotoxicity assays

Compounds	Assay	IC_{50} (μM)	Ref
		MCF-7	
$[Cu(L)_2SO_4]$	SRB	66.90	[41]
$[Cu(L)_2Cl_2]$	SRB	52.80	
$[Cu(L)_2]$	MTT	56.00	[42]
$[Cu(L)_2]$	MTT	19.37	[36]
$[Cu(L)]\cdot 3H_2O$	XTT	62.20	[43]
$[Cu(L)(NO_3)(OH_2)_2]$	DPPH	6.13 ± 0.3	[44]
CuBBr	MTT	370.60	This work
$CuBOCH_3$	MTT	27.60	This work
$CuBNO_2$	MTT	17.76	This work

their concentration. It is observed that the R-value close to 1 signifies a high correlation between the complex's effectiveness and its concentration.

The cytotoxicity of the synthesized Cu(II) complexes was evaluated and compared with previously reported Cu(II) complexes presented in Table 15. The IC_{50} values for CuBBr, $CuBOCH_3$, and $CuBNO_2$ were 370.60, 27.60, and 17.76 μM, respectively. Notably, $CuBNO_2$ exhibited the highest cytotoxicity among the synthesized complexes, showing a significantly lower IC_{50} than $CuBOCH_3$ and CuBBr. When compared to previous studies, certain Cu(II) complexes such as $[Cu(L)_2]$ (IC_{50} = 19.37 μg/mL) [3] and $[Cu(L)_2Cl_2]$ (IC_{50} = 52.8 μM) demonstrated strong cytotoxic effects. However, differences in IC_{50} values may arise due to variations in ligand structures, coordination environments, and assay methods. The presence of electron-withdrawing ($-NO_2$) and electron-donating ($-OCH_3$) groups in the ligands influenced the cytotoxicity of the synthesized complexes, with $CuBNO_2$ showing the highest potency. Moreover, the use of different assays, such as MTT, SRB, DPPH, and XTT, introduces variability in IC_{50} measurements, as each assay evaluates cytotoxicity through distinct cellular mechanisms. These findings suggest that ligand modification plays a critical role in tuning the biological activity of Cu(II) complexes, and further structural optimizations may enhance their anticancer potential.

■ CONCLUSION

This study synthesized three Schiff base ligands derived from 2-hydroxynaphthaldehyde, and three azo dye ligands derived from 2-naphthol using various substituted aniline derivatives as coupling agents. The prepared ligands were characterized using ^{13}C-NMR, ^{1}H-NMR, and FTIR techniques. These six ligands were then used to prepare copper complexes in an ethanol medium in a 1:2 (M:L) ratio. The characterization data of the prepared complexes indicates that the geometric shape of the prepared copper complexes is square planar. The biological activity results showed that the copper complexes significantly affect cancer cells, and their ability to inhibit cancer cell growth occurs with varying effectiveness. Statistical analysis of IC_{50} results shows that copper complexes CuABr, CuBBr, and $CuAOCH_3$ have a higher effect on cancer cells compared to healthy cells, with highly significant differences. In comparison, complexes $CuBOCH_3$ and $CuBNO_2$ have a higher impact on cancer cells than healthy cells with substantial differences. However, the $CuANO_2$ complex had a higher effect on normal cells than cancer cells.

■ CONFLICT OF INTEREST

The authors declare no conflict of interest.

■ AUTHOR CONTRIBUTIONS

Haneen Fadhil Abbas: formal analysis, data curation and writing – original draft preparation. Faris Jassim Aldoghachi: supervision and writing – reviewing and editing. Basil Abdulmahdi Saleh: validation and conceptualization. Yun Hin Taufiq-Yap: validation and conceptualization.

■ REFERENCES

[1] Ansari, M.F., Khan, H.Y., Tabassum, S., and Arjmand, F., 2023, Advances in anticancer alkaloid-derived metallo-chemotherapeutic agents in the last decade: Mechanism of action and future prospects, *Pharmacol. Ther.*, 241, 108335.

[2] Ji, P., Wang, P., Chen, H., Xu, Y., Ge, J., Tian, Z., and

Yan, Z., 2023, Potential of copper and copper compounds for anticancer applications, *Pharmaceuticals*, 16 (2), 234.

[3] Molinaro, C., Martoriati, A., Pelinski, L., and Cailliau, K., 2020, Copper complexes as anticancer agents targeting topoisomerases I and II, *Cancers*, 12 (10), 2863.

[4] Al-Khazraji, A.M.A., 2024, Synthesis, Characterization, and evaluation of MCF-7 (breast cancer) for Schiff, Mannich bases, and their complexes, *Indones. J. Chem.*, 24 (1), 213–227.

[5] Wang, C., Yang, X., Dong, C., Chai, K., Ruan, J., and Shi, S., 2023, Cu-related agents for cancer therapies, *Coord. Chem. Rev.*, 487, 215156.

[6] Maher, K., 2018, Schiff bases derived from 2-hydroxynaphthalene-1-carbaldehyde and their metal complexes: A review, *Asian J. Chem.*, 30 (6), 1171–1182.

[7] Abbas, H.F., Saleh, B.A., Al-Doghachi, F.A.J., Kariuki, B.M., and El-Hiti, G.A., 2025, Crystal structure of *bis* ((1-((*E*)-((4-methoxyphenyl)imino)methyl)naphthalen-2-yl)oxy) copper(II), $C_{36}H_{28}CuN_2O_4$, *Z. Kristallogr. - New Cryst. Struct.*, 240 (2), 247–249.

[8] Ashrafuzzaman, M.D., Camellia, F.K., Al Mahmud, A., Pramanik, M.D.J., Nahar, K., Haque, M.M., and Kudrat-E-Zahan, M., 2021, Bioactive mixed ligand metal complexes of Cu(II), Ni(II), and Zn(II) ions: Synthesis, characterization, antimicrobial and antioxidant properties, *J. Chil. Chem. Soc.*, 66 (3), 5295–5299.

[9] Kyhoiesh, H.A.K., and Al-Adilee, K.J., 2021, Synthesis, spectral characterization, antimicrobial evaluation studies and cytotoxic activity of some transition metal complexes with tridentate (N,N,O) donor azo dye ligand, *Results Chem.*, 3, 100245.

[10] Akhter, S., Ul Zaman, H., Mir, S., Dar, A.M., and Shrivastava, S., 2017, Synthesis of Schiff base metal complexes: A concise review, *Eur. Chem. Bull.*, 6 (10), 475–483.

[11] Shi, S., Yu, S., Quan, L., Mansoor, M., Chen, Z., Hu, H., Liu, D., Liang, Y., and Liang, F., 2020, Synthesis and antitumor activities of transition metal complexes of a bis-Schiff base of 2-hydroxy-1-naphthalenecarboxaldehyde, *J. Inorg. Biochem.*, 210, 111173.

[12] Athira, L.S., Balachandran, S., and Sudha Devi, R., 2019, Synthesis, crystal structure, solvatochromic properties and DNA cleaving activity of azo derivative of naphthalen-2-ol, *J. Mol. Struct.*, 1180, 100–109.

[13] Kareem, M.A., and Salman, H.D., 2017, Synthesis, characterization and antimicrobial studies of Transition metal complexes with azo ligand derivative from 4-aminoantipyrine, *Mesopotamia Environ. J.*, Special Issue C, 83–91.

[14] Gaber, M., Hassanein, A.M., and Lotfalla, A.A., 2008, Synthesis and characterization of Co(II), Ni(II) and Cu(II) complexes involving hydroxy antipyrine azodyes, *J. Mol. Struct.*, 875 (1-3), 322–328.

[15] Vinodkumar, V., and Keshavayya, J., 2019, Synthesis, structural investigations and *in vitro* biological evaluation of *N*,*N*-dimethyl aniline derivatives based azo dyes as potential pharmacological agents, *J. Mol. Struct.*, 1186, 404–412.

[16] Ajani, O.O., Akinremi, O.E., Ajani, A.O., Edobor-Osoh, A., and Anake, W.U., 2013, Synthesis and spectroscopic study of naphtholic and phenolic azo dyes, *Phys. Rev. Res. Int.*, 3 (1), 28–41.

[17] Nagesh, G.Y., and Mruthyunjayaswamy, B.H.M., 2015, Synthesis, characterization and biological relevance of some metal (II) complexes with oxygen, nitrogen and oxygen (ONO) donor Schiff base ligand derived from thiazole and 2-hydroxy-1-naphthaldehyde, *J. Mol. Struct.*, 1085, 198–206.

[18] Xue, S., Xie, Z., and He, J., 2021, 1-[(2-Hydroxy-phenylimino)-methyl]-naphthalen-2-ol: Application in detection and adsorption of aluminum ions, *Res. Chem. Intermed.*, 47 (10), 4333–4347.

[19] Aiyelabola, T., Akinkunmi, E., Obuotor, E., Olawuni, I., Isabirye, D., and Jordaan, J., 2017, Synthesis characterization and biological activities of coordination compounds of 4-hydroxy-3-nitro-

2*H*-chromen-2-one and its aminoethanoic acid and pyrrolidine-2-carboxylic acid mixed ligand complexes, *Bioinorg. Chem. Appl.*, 2017 (1), 6426747.

[20] Gündüz, H.M., and Bilgiç, S., 2011, Electrophilic aromatic iodine substitution of 1-[(*p*-tolylimino)methyl]-naphthalen-2-ol in zeolite catalyst, *Sakarya Univ. J. Sci.*, 15 (2), 121–128.

[21] Ahmed, F., Dewani, R., Pervez, M.K., Mahboob, S.J., and Soomro, S.A., 2016, Non-destructive FT-IR analysis of mono azo dyes, *Bulg. Chem. Commun.*, 48 (1), 71–77.

[22] Gavranić, M., Kaitner, B., and Meštrović, E., 1996, Intramolecular N−H...O hydrogen bonding, quinoid effect, and partial π-electron delocalization in N-aryl Schiff bases of 2-hydroxy-1-naphthaldehyde: The crystal structures of planar *N*-(α-naphthyl)- and *N*-(β-naphthyl)-2-oxy-1-naphthaldimine, *J. Chem. Crystallogr.*, 26 (1), 23–28.

[23] Elemike, E.E., Nwankwo, H.U., Onwudiwe, D.C., and Hosten, E.C., 2017, Synthesis, crystal structures, quantum chemical studies and corrosion inhibition potentials of 4-(((4-ethylphenyl)imino)methyl)phenol and (*E*)-4-((naphthalen-2-ylimino) methyl) phenol Schiff bases, *J. Mol. Struct.*, 1147, 252–265.

[24] Sagar, S., Parween, A., Mandal, T.K., Lewis, W., and Naskar, S., 2020, Mn(IV), Co(II) and Ni(II) complexes of the Schiff bases of 2-hydroxy-naphthaldehyde with amino alcohols: Synthesis, characterization and electrochemical study; DFT study and Catecholase activity of Mn(IV) complex, *J. Coord. Chem.*, 73 (20-22), 2919–2940.

[25] Nassir, K.M., El-ghamry, M.A., Elzawawi, F.M., Abdel Aziz, A.A., and Abu-El-Wafa, S.M., 2020, Novel nano Schiff base M(II) and M(III) complexes derived from antiviral valacyclovir and 2-hydroxy-1-naphthaldehyde (HNAPB). Structural characterization, bio-efficiency, DNA interaction, molecular modeling, docking and conductivity studies, *IOSR J. Appl. Chem.*, 13 (5), 1–25.

[26] Sujamol, M.S., Athira, C.J., Sindhu, Y., and Mohanan, K., 2021, Synthesis, spectroscopic characterization, dyeing performance and corrosion inhibition study of transition metal complexes of a novel azo derivative formed from 2-aminothiophene, *Chem. Data Collect.*, 31, 100634.

[27] Manimaran, P., Balasubramaniyan, S., Azam, M., Rajadurai, D., Al-Resayes, S.I., Mathubala, G., Manikandan, A., Muthupandi, S., Tabassum, Z., and Khan, I., 2021, Synthesis, spectral characterization and biological activities of Co(II) and Ni(II) mixed ligand complexes, *Molecules*, 26 (4), 823.

[28] Jia, W.G., Wang, Z.B., Zhi, X.T., Han, J.Q., and Sun, Y., 2017, Syntheses, characterization and catalytic activities of half-sandwich ruthenium complexes with naphthalene-based Schiff base ligands, *J. Coord. Chem.*, 70 (5), 848–858.

[29] Chetioui, S., Zouchoune, B., Merazig, H., Bouaoud, S.E., Rouag, D., and Djukic, J.P., 2021, Synthesis, spectroscopic characterization, crystal structure and theoretical investigation of two azo-palladium (II) complexes derived from substituted (1-phenylazo)-2-naphtol, *Transition Met. Chem.*, 46 (2), 91–101.

[30] Kadafour, A.N.W., and Bala, M.D., 2022, Crystal structure of (E)-1-(((3-nitrophenyl)imino)methyl)naphthalen-2-ol, *Crystallogr. Rep.*, 67 (2), 214–217.

[31] Ferreira, G.R., and de Oliveira, L.F.C., 2017, Synthesis, spectroscopic and structural studies of new azo dyes metal chelates derivated from 1-phenil-azo-2-naphthol, *J. Mol. Struct.*, 1146, 50–56.

[32] Satheesh, C.E., Raghavendra Kumar, P., Suchetan, P.A., Rajanaika, H., and Foro, S., 2021, New (N,O) Schiff bases of 2-hydroxynaphthaldehyde and their homoleptic Zn(II) and Cu(II) complexes – Synthesis, structural characterization, Hirshfeld surface analysis and antimicrobial activity studies, *Inorg. Chim. Acta*, 515, 120017.

[33] Ran, X., Wang, L., Lin, Y., Hao, J., and Cao, D., 2010, Syntheses, characterization and biological studies of zinc(II), copper(II) and cobalt(II) complexes with Schiff base ligand derived from 2-hydroxy-1-naphthaldehyde and selenomethionine, *Appl. Organomet. Chem.*, 24 (10), 741–747.

[34] El-Tabl, A.S., Mohamed Abd El-Waheed, M., Wahba, M.A., and Abd El-Halim Abou El-Fadl, N.,

2015, Synthesis, characterization, and anticancer activity of new metal complexes derived from 2-hydroxy-3-(hydroxyimino)-4-oxopentan-2-ylidene)benzohydrazide, *Bioinorg. Chem. Appl.*, 2015 (1), 126023.

[35] Mukherjee, S., Pal, C.K., Kotakonda, M., Joshi, M., Shit, M., Ghosh, P., Choudhury, A.R., and Biswas, B., 2021, Solvent induced distortion in a square planner copper(II) complex containing an azo-functionalized Schiff base: Synthesis, crystal structure, *in-vitro* fungicidal and anti-proliferative, and catecholase activity, *J. Mol. Struct.*, 1245, 131057.

[36] Al-Salim, Y.M., and Al-Asadi, R.H., 2023, Synthesis, anti-breast cancer activity, and molecular docking studies of thiourea benzamide derivatives and their complexes with copper ion, *Trop. J. Nat. Prod. Res.*, 7 (6), 3158–3167.

[37] Kazakova, R.R., and Masson, P., 2022, Quantitative measurements of pharmacological and toxicological activity of molecules, *Chemistry*, 4 (4), 1466–1474.

[38] Nasser, A.T., and Al-Asadi, R., 2023, Schiff bases ligands derived from *o*-phthalaldehyde and their metal complexes with Cu^{2+} and Ni^{2+}: Synthesis, anti-breast cancer and molecular docking study, *Trends Sci.*, 20 (9), 5675.

[39] Berrouet, C., Dorilas, N., Rejniak, K.A., and Tuncer, N., 2020, Comparison of drug inhibitory effects (IC_{50}) in monolayer and spheroid cultures, *Bull. Math. Biol.*, 82 (6), 68.

[40] Abbas, H.H., Al-Luaibi, M.Y., and Al-Assadi, M.J., 2023, New heterocyclic organo-chalcogenide compounds: Synthesis, physicochemical characterization, and evaluation of anticancer activity against breast cancer cells, *Indones. J. Chem.*, 23 (2), 309–320.

[41] Chandra, S., Vandana, V., and Kumar, S., 2015, Synthesis, spectroscopic, anticancer, antibacterial and antifungal studies of Ni(II) and Cu(II) complexes with hydrazine carboxamide, 2-[3-methyl-2-thienyl methylene], *Spectrochim. Acta, Part A*, 135, 356–363.

[42] Rambabu, A., Pradeep Kumar, M., Ganji, N., Daravath, S., and Shivaraj, S., 2020, DNA binding and cleavage, cytotoxicity and antimicrobial studies of Co(II), Ni(II), Cu(II) and Zn(II) complexes of 1-((E)-(4-(trifluoromethoxy)phenylimino)methyl) naphthalen-2-ol Schiff base, *J. Biomol. Struct. Dyn.*, 38 (1), 307–316.

[43] Sahan, F., Kose, M., Hepokur, C., Karakas, D., and Kurtoglu, M., 2019, New azo-azomethine-based transition metal complexes: Synthesis, spectroscopy, solid-state structure, density functional theory calculations and anticancer studies, *Appl. Organomet. Chem.*, 33 (7), e4954.

[44] El-Gammal, O.A., Mohamed, F.Sh., Rezk, G.N., and El-Bindary, A.A., 2021, Structural characterization and biological activity of a new metal complexes based of Schiff base, *J. Mol. Liq.*, 330, 115522.